ISSN 2618-1584 Vol. 4, Issue 10: 49-55, DOI: 10.25236/FMSR.2022.041009

Differential Diagnosis of Benign and Malignant Breast Tumors Based on DCE-MRI

Xuan Ren, Menghua Chen, Ruijie Du, Weijie Xing

School of Health Science and Engineering, University of Shanghai for Science and Technology, 516 Jungong Road, Yangpu, 200093, Shanghai, China

Abstract: *Breast cancer is a malignant tumor mostly found in the female population, and it is important to improve the survival rate of patients by determining its benignity and malignancy at the early stage of the disease through non-invasive imaging, so that appropriate treatment can be adopted. In this paper, we tested the application of the deep learning model of residual network (Resnet) in the diagnosis of breast tumors by Dynamic Contrast-Enhanced MRI (DCE-MRI), and compared three network models of different depths, Resnet50, Resnet34, and Resnet18, to find the best way to achieve the diagnosis of breast tumors. With the number of network layers increasing the depth of the network increases, and the phenomenon of overfitting occurs. The results showed that Resnet18 was the most accurate method to classify benign and malignant tumor images. The experimental results showed that the accuracy of Resnet18 network was higher, reaching 96.4%.*

Keywords: *tumor of breast, Benign and malignant classification, Resnet*

1. Introduction

Breast cancer, known as the "pink killer", is a malignant tumor that occurs most frequently in women and has the highest incidence rate among female cancers [1]. According to the 2020 Global Cancer Data released by the International Agency for Research on Cancer (IARC) of the World Health Organization, 2.3 million women were diagnosed with breast cancer worldwide, and 685,000 of them died. The number of new cases of breast cancer reached 2.26 million compared to 2.21 million for lung cancer, and breast cancer officially replaced lung cancer as the number one cancer worldwide [2][3]. Although the incidence and mortality rate of breast cancer among women in China is still at a low level in the world, it has been increasing rapidly in recent years because of the large population base in China [4]. Early detection, early diagnosis, and early treatment can effectively improve the survival rate of breast cancer patients.

Currently, the main imaging methods used to screen for breast cancer disease are mammography, ultrasound, and magnetic resonance imaging (MRI) [5]. Among these methods, MRI is more widely used in breast cancer screening because of its richer image information, higher tissue resolution, and no damage to the body. Dynamic Contrast-Enhanced MRI (DCE-MRI) not only shows the morphological details of tumor lesions, but also provides hemodynamic signs of signal changes in the lesion area, such as the early enhancement rate and the percentage of extravascular interstitial volume. These provide an important basis for the initial clinical diagnosis.

Nowadays, most of the early diagnosis of breast cancer is still made by imaging physicians reading the scanned images to initially determine whether there is a lesion in the breast, and to initially determine the benignity or malignancy of the lump according to the morphological characteristics of the image. However, this early screening mainly relies on the physician's own a priori knowledge and subjective judgment, and with the increasing number of imaging data in recent years, the amount of films read by imaging physicians has increased, which makes it easy to miss or misdiagnose the disease, resulting in patients not receiving timely treatment [6]. Computer-Aided Diagnosis (CAD) systems can provide physicians with complementary advice in detecting lesions and diagnosing them, improving efficiency and diagnostic accuracy [7].

At present, there are two ways to apply CAD in breast cancer diagnosis: one is breast cancer image diagnosis by manual feature extraction and traditional machine learning; the other is breast cancer image diagnosis based on deep learning. Compares to the traditional machine learning, the deep learning model can automatically extract features from images, and with the deepening of a convolutional network, it can recognize more abstract and high-dimensional features, which is more effective and widely used.

ISSN 2618-1584 Vol. 4, Issue 10: 49-55, DOI: 10.25236/FMSR.2022.041009

In 2013, Yan Liu from Harbin Institute of Technology used breast Doppler ultrasound images to build a classifier using a support vector machine (SVM) approach to achieve 88.18% accuracy for benign and malignant breast tumors [8].In 2014, Gorge et al. proposed an intelligent remote detection and diagnosis system for breast cancer, trained with different machine learning methods, and achieved an accuracy of 92 breast cytology images containing 11,502 nuclei with 84% to 96% accuracy [9].In 2017 Mei Sun et al. used hybrid features combined with a random forest algorithm to classify breast tumor ultrasound images and achieved an average accuracy of 79% [10]. The S-Detect artificial intelligence system is a set of assisted ultrasound imaging for a diagnostic deep learning system that system extracts morphological features from the American College of Radiology (BI-RADS) recommended breast image reporting data system. In 2021, Xia et al. used the S-Detect artificial intelligence system to classify 40 cases in an experiment and achieved an accuracy of 89.16% [11].

In recent years, Convolutional Neural Networks (CNN) has achieved excellent results in image classification and have made great progress in areas such as medical images. At present, the main convolutional neural network models are VGGNet, Le Net, Google Net, Resnet, and so on. Among them, the residual network (Resnet), which was proposed by Kaiming He et al. in 2015, has the characteristics of deeper network depth, no gradient disappearance phenomenon, higher accuracy in image classification, and solves the problem of deep network degradation to some extent [12].

In this paper, we explored the application of deep learning models applying residual networks in the diagnosis of benign and malignant breast cancer by DCE-MRI to achieve higher accuracy in predicting benign and malignant breast tumors.

2. Data set

The data collected in this study were all from Xinhua Hospital affiliated with Shanghai Jiao Tong University School of Medicine, and after the screening, the image images of 154 patients were finally selected as the data set, including 46 benign and 108 malignant cases, and each patient had MRI images of five phases from S0 to S4, as well as one pathology report.

Inclusion criteria: (1) no cardiac or pulmonary disorders; (2) no treatment before DCE-MRI examination; (3) MRI images with artifacts and no obvious motion were excluded; (4) DCE-MRI examination was performed first, and pathological results were obtained after puncture or surgery.

Exclusion criteria: (1) puncture, surgery, or adjuvant chemotherapy prior to DCE-MRI; (2) incomplete imaging or pathology reports; (3) small breast lesions (<10 mm) that make it difficult to outline the region of interest (ROI) of the lesion.

2.1. Image data acquisition

The Philips Ingenia 3.0T superconducting MR equipment was used, and the patient was examined in a prone position with both breasts draped in a phased array coil. An appropriate pressure was applied to fix the breasts in a nipple-down position for imaging. In the raw image data acquired in this study, the dynamic-enhanced T1 high-resolution isotropic volume excitation (dyn-eTHRIVE) enhancement scan was set for five temporal phases of the scan, S0 to S4, respectively. The settings were different for each patient's scan, so the S-phases had varying amplitudes of 150, 170, and 180, but the amplitudes were the same between different S-phases of the same patient.

2.2. Dataset processing

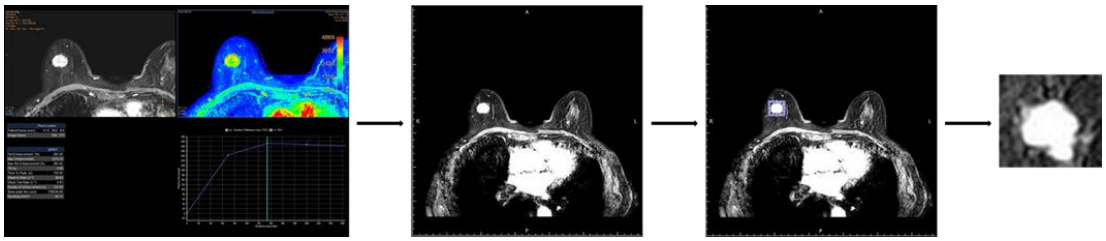

Figure 1: Image processing flow chart

The images of the patient's breast masses were segmented using MATLAB software under the supervision of the imaging physician, taking into account the physician's experience and the patient's

ISSN 2618-1584 Vol. 4, Issue 10: 49-55, DOI: 10.25236/FMSR.2022.041009

actual condition. The crop size was moderately scaled in order to encompass the lesion in its entirety.

2.3. Image enhancement

Gaussian filtering is performed on the cropped image pictures. Gaussian filter is a linear filter that can effectively suppress noise and smooth the image, which is widely used in the noise reduction process of image processing [13]. The one-dimensional form of the Gaussian distribution function is as follows.

$$G(x) = \frac{1}{\sqrt{2\pi}\sigma} e^{-\frac{x^2}{2\sigma^2}} \tag{1}$$

Where the magnitude of σ determines the width of the Gaussian function. Two-dimensional forms are commonly used in image processing.

$$G(x, y) = \frac{1}{2\pi\sigma^2} e^{-\frac{x^2+y^2}{2\sigma^2}} \tag{2}$$

Gaussian filtering enhancement of images before they are fed into the deep learning training model can effectively eliminate noise and improve the accuracy of training.

3. Model Introduction

3.1. Convolution Neural Network [14]

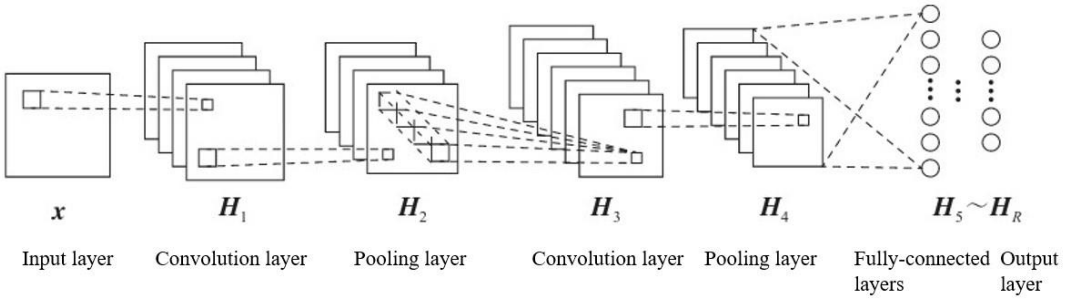

Figure 2: Schematic diagram of convolutional neural network

Input layer: In image processing, the input layer generally represents a three-dimensional pixel matrix of an image, usually of size w×h×3 or w×h×1, where the three dimensions are the width, length, and depth of the image. The depth is also called the number of channels. The image in this paper is a black and white image with the only one-color channel.

Convolution layer: obtains the local area features of the image by a convolution operation.

Pooling layer: The pooling layer, also called the lower sampling layer, which is generally placed among successive convolutional layers, and its role is to reduce the feature map, and retain useful information, and get a smaller submap to characterize the original image. The pooling operation is essentially the lower sampling of the image, which can be regarded as transforming a high-resolution image into a lower-resolution subgraph, with the retained subgraph not having much impact on the understanding of the image content.

Fully-connected layers: After multiple layers of convolutional and pooling operations, there are usually 1-2 fully-connected layers that give the final classification results. The fully-connected layer acts as a "classifier" in the whole convolutional neural network, mapping the learned feature representations to the class label space.

3.2. Deep residual network (Resnet)

For a stacked-layer structure, the learned features are denoted as H(x) when the input is H(x) and the residual F(x) = H(x) – x so that the original learned features are actually F(x) + x.

ISSN 2618-1584 Vol. 4, Issue 10: 49-55, DOI: 10.25236/FMSR.2022.041009

The residual learning is easier than the original feature learning directly. When the residual is 0, the stacking layer only does constant mapping, but at least the network performance will not degrade. In fact, the residual will not be 0, which also makes the stacking layer to learn new features based on the input features, and thus have better performance. The structure of residual learning is shown in the figure below, similar to the "short circuit" in the circuit. Therefore, it is a shortcut connection.

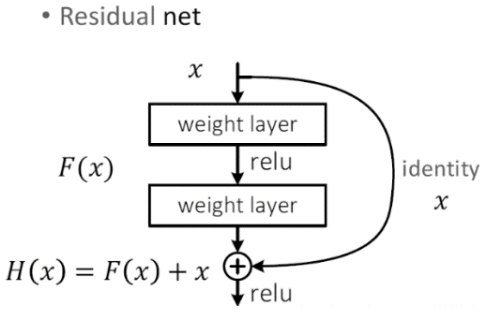

Figure 3: Schematic diagram of shortcut connection

There are some differences in the structure of the nets at different depths, as shown in the table below.

Table 1: Some differences in the structure of the nets at different depths

Layer name	Output size	Resnet 50	Resnet 34	Resnet 18
Conv1	112×112	7×7, 64, stride 2		
		3×3 max pool, stride 2		
Conv2_x	56×56	$\begin{bmatrix}1\times1 & 64\\ 3\times3 & 64\\ 1\times1 & 256\end{bmatrix}\times3$	$\begin{bmatrix}3\times3 & 64\\ 3\times3 & 64\end{bmatrix}\times3$	$\begin{bmatrix}3\times3 & 64\\ 3\times3 & 64\end{bmatrix}\times2$
Conv3_x	28×28	$\begin{bmatrix}1\times1 & 128\\ 3\times3 & 128\\ 1\times1 & 512\end{bmatrix}\times4$	$\begin{bmatrix}3\times3 & 128\\ 3\times3 & 128\end{bmatrix}\times4$	$\begin{bmatrix}3\times3 & 128\\ 3\times3 & 128\end{bmatrix}\times2$
Conv4_x	14×14	$\begin{bmatrix}1\times1 & 256\\ 3\times3 & 256\\ 1\times1 & 1024\end{bmatrix}\times6$	$\begin{bmatrix}3\times3 & 256\\ 3\times3 & 256\end{bmatrix}\times6$	$\begin{bmatrix}3\times3 & 256\\ 3\times3 & 256\end{bmatrix}\times2$
Conv5_x	7×7	$\begin{bmatrix}1\times1 & 512\\ 3\times3 & 512\\ 1\times1 & 2048\end{bmatrix}\times3$	$\begin{bmatrix}3\times3 & 512\\ 3\times3 & 512\end{bmatrix}\times3$	$\begin{bmatrix}3\times3 & 512\\ 3\times3 & 512\end{bmatrix}\times2$
	1×1	Average pool, 256-d fc, softmax		
FLOPS		3.8×10^9	3.6×10^9	1.8×10^9

4. Result

The CPU of the model training device designed in this paper is Core 19-9900KF and the GPU is Nvidia RTX2080Ti. The model is built based on Pytorch and trained in Pycharm, using resnet50, resnet34, and resnet18 models respectively. The procedure sets the program to randomly divide the dataset into training and test sets according to 7:3 randomly. When the loss of the test set stops improving, the learning rate is reduced, and 0.2 is the ratio of each decrease. During the training process, the learning rate was reduced when the index did not improve for 5 times in a row, and a total of 30 iterations were performed.

In order to evaluate the accuracy of the prediction of tumor benignity and malignancy under different frameworks, each type of model was evaluated separately in this paper, and the evaluation indexes were Accuracy (ACC), Receiver Operating Characteristic Curve (ROC), Area Under Curve (AUC), and Area Under Curve (AUC). Area Under Curve (AUC).

The accuracy rate was calculated as follows.

$$Acc = \frac{TP + TN}{TP + TN + FP + FN} \tag{3}$$

Where TP refers to the number of samples with malignant label and predicted outcome; TN refers to the number of samples with benign label and predicted outcome; FP refers to the number of samples with the benign label but predicted outcome, and FN refers to the number of samples with the malignant label

ISSN 2618-1584 Vol. 4, Issue 10: 49-55, DOI: 10.25236/FMSR.2022.041009

but predicted outcome.

AUC is the area enclosed by the ROC curve and the coordinate axis, which can reflect the comprehensive performance of the classification network. The horizontal coordinate of the ROC curve is the False Positive Rate (FPR), which is calculated as shown in Equation (4), and the vertical coordinate is the True Positive Rate (TPR), which is calculated as shown in Equation (5).

$$FPR = \frac{FP}{TN + FP} \tag{4}$$

$$TPR = \frac{TP}{TP + FN} \tag{5}$$

The training results of the model on the test set are shown in the following table.

Table 2: The training results of the model on the test set

	Resnet 50	Resnet 34	Resnet 18
Accuracy	0.723	0.784	0.964
AUC	0.799	0.845	0.942

The ROC curve is shown in the figure below.

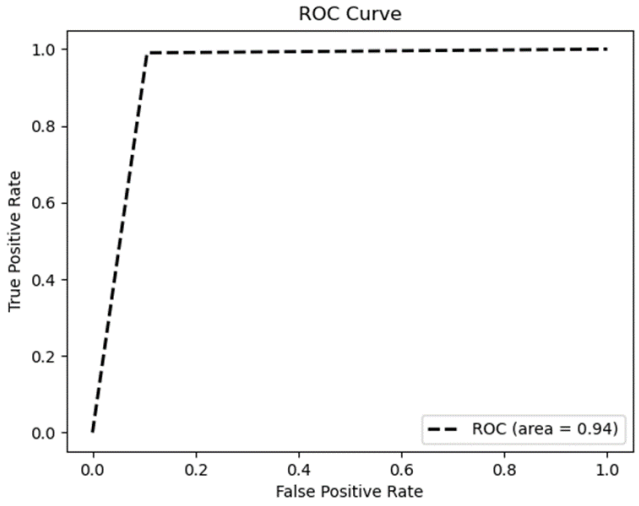

Figure 4: ROC Curve

The accuracy of the training results in this paper is compared with other experiments as follows.

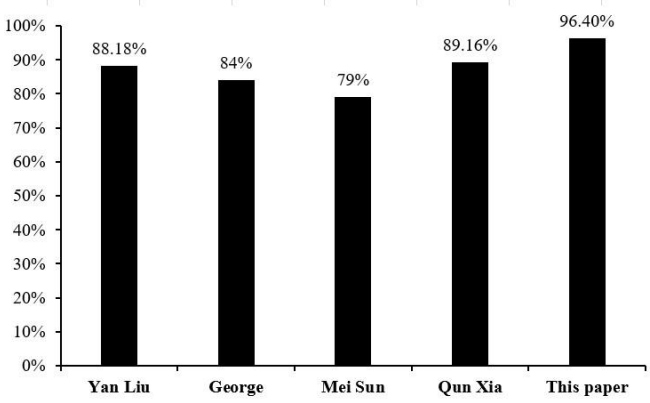

Figure 5: Compared with the accuracy of others' methods

5. Discussion

The causes of breast cancer are not fully researched. Therefore, the accurate means of prevention are

ISSN 2618-1584 Vol. 4, Issue 10: 49-55, DOI: 10.25236/FMSR.2022.041009

lacking. A large number of scientific studies have shown that early breast cancer is not incurable, and the diagnosis of the benignity and malignancy of breast lumps at the early stage of disease detection plays an extremely important role in the selection of subsequent treatment methods and the improvement of survival rate of patients. With the continuous improvement of medical treatment, the examination and diagnosis of breast cancer have developed into mainstream methods such as palpation, biopsy, and breast imaging observation. The palpation method is based mostly on the clinician's experience, which is comparatively more subjective. The biopsy is an invasive examination, which can cause some physical and psychological harm to patients. Besides, imaging is one of the most popular methods today because it can greatly improve the accuracy of results while not harming the human body.

This paper presents a study related to the classification of benign and malignant masses present in breast DCE-MRI images based on deep learning methods. The accuracy of different depth models Resnet50, Resnet34, and Resnet18 for benign and malignant classification was compared by designing classification training models. The cropped lump images were smaller and the shallow neural network model worked better. The reason why is that with the increase of network layers, the phenomenon of over-fitting appears in the deep learning training of cropped images, which leads to a decrease in accuracy with greater depth. Compared to others in differentiating benign and malignant breast tumors, the accuracy of the Resnet18t network model used in this study is higher. It was confirmed by the experimental results that the network structure of Resnet18 had a higher accuracy of 96.4% in comparison.

This model has better results for benign malignancy classification of breast cancer and it is a potential application in breast cancer prediction in the medical industry, which is expected to relieve clinicians' pressure of reading films and it is beneficial to assist them in diagnosis, and finding treatments for patients.

References

[1] Siegel RL, Miller KD, Fuchs HE, Jemal A. Cancer statistics, 2022. CA Cancer J Clin. 2022 Jan;72(1):7-33. doi: 10.3322/caac.21708. Epub 2022 Jan 12. PMID: 35020204.

[2] Global Cancer Statistics Report 2020[J]. Chinese Journal of Preventive Medicine,2021,55(03):398-398.

[3] Liu Zongchao, LI Zhexuan, ZHANG Yang, ZHOU Tong, ZHANG Jingying, You Weicheng, Pan Kaifeng, LI Wenqing. Interpretation on the report of Global Cancer Statistics 2020[J]. Journal of Multidisciplinary Cancer Management (Electronic Version),2021,7(02):1-14.

[4] Zhang Yacong, LV Zhangyan, SONG Fangfang, Chen Kexin. Trends in incidence and mortality of breast cancer worldwide and in China[J]. Journal of Multidisciplinary Cancer Management (Electronic Version),2021,7(02):14-20.

[5] Yubei Huang, Zhongsheng Tong, Kexin Chen, Ying Wang, Peifang Liu, Lin Gu, Juntian Liu, Jinpu Yu, Fengju Song, Wenhua Zhao, Yehui Shi, Hui Li, Huaiyuan Xiao, Xishan Hao. Interpretation of guideline for breast cancer screening in Chinese women[J]. Chinese Journal of Clinical Oncology, 2019, 46(09):432-440.

[6] Yang Lei, Tang Can. CAD machine diagnosis system in ultrasonic diagnosis of breast cancer [J]. The Journal of Practical Medicine, 2022,38(01):106-110.

[7] Nie Shengdong, Wei Chuanling, Zhang Xiaobing. Review of breast cancer computer-aided detection methods based on magnetic resonance imaging [J/OL]. Journal of University of Shanghai for Science and Technology:1-11[2022-03-16].DOI:10.13255/j.cnki.jusst.20211225001.

[8] Liu Yan. RESEARCH ON KEY TECHNOLOGIES OF BENIGN AND MALIGNANT CLASSIFICATION BASED ON DUAL-MODE BREAST ULTRASOUND IMAGES [D]. Harbin Institute of Technology, 2013.

[9] George Y M, Zayed H H, Roushdy M I, et al. Remote Computer-Aided Breast Cancer Detection and Diagnosis System Based on Cytological Images [J]. IEEE Systems Journal, 2014, 8(3):949-964.

[10] Sun Mei, Yan Chuanbo, Zhang Yu, Bi Xuehua. Optimization and Classification of Ultrasound Image Features for Breast Tumors Based on Data Mining Algorithm [J]. Bulletin of Science and Technology, 2017, 33(10): 67-72. DOI: 10.13774/j.cnki.kjtb.2017.10.013.

[11] Qun Xia, Yangmei Cheng, Jinhua Hu, Juxia Huang, Yi Yu, Hongjuan Xie, Jun Wang.Differential diagnosis of breast cancer assisted by S-Detect artificial intelligence system [J].Mathematical Biosciences and Engineering, 2021,18(4):3680-3689.doi: 10.3934/mbe.2021184

[12] H. -C. Shin et al., "Deep Convolutional Neural Networks for Computer-Aided Detection: CNN Architectures, Dataset Characteristics and Transfer Learning," in IEEE Transactions on Medical Imaging, vol. 35, no. 5, pp. 1285-1298, May 2016, doi: 10.1109/TMI.2016.2528162.

[13] Nurwahidah Mamat, Wan Eny Zarina Wan Abdul Rahman, Shaharuddin Soh, Rozi Mahmud (2016). Evaluation of Performance for Different Filtering Methods in CT Brain Images. AIP Conference

ISSN 2618-1584 Vol. 4, Issue 10: 49-55, DOI: 10.25236/FMSR.2022.041009

Proceedings. https://doi.org/10.1063/1.5055479
[14] Jose Bernal, Kaisar Kushibar, Daniel S. Asfaw, Sergi Valverde, Arnau Oliver, Robert Mart í, Xavier Llad ó, Deep convolutional neural networks for brain image analysis on magnetic resonance imaging: a review, Artificial Intelligence in Medicine, Volume 95,2019, Pages 64-81,ISSN 0933-3657.
[15] Yu Dong. Benign and Malignant Classification of Nodules in Mammography Images [D]. Huazhong University of Science and Technology. 2020.